Ultra-lightweight rechargeable battery: >750 Wh/kg lithium–sulfur pouch cell

Masaki Kakiage (✉ kakiage@gunma-u.ac.jp)

Gunma University   https://orcid.org/0000-0002-5396-6189

Kenji Kakiage

ADEKA CORPORATION

Toru Yano

ADEKA CORPORATION

Hiroki Uehara

Gunma University

Article

Keywords:

Additional Declarations: There is **NO** Competing Interest.

Ultra-lightweight rechargeable battery: >750 Wh/kg lithium–sulfur pouch cell

Kenji Kakiage[1]*, Toru Yano[1], Hiroki Uehara[2] and Masaki Kakiage[2]*

[1] Environmental & Energy Materials Laboratory, ADEKA Corporation, 7-2-35 Higashi-ogu, Arakawa-ku, Tokyo 116-8554, Japan

[2] Division of Molecular Science, Graduate School of Science and Technology, Gunma University, 1-5-1 Tenjin-cho, Kiryu, Gunma 376-8515, Japan

Abstract

Lithium–sulfur (Li–S) rechargeable batteries have been expected to be lightweight energy storage devices with the highest gravimetric energy density at the single-cell level reaching up to 695 Wh/kg-cell (a low rate of 0.005C, only in the first discharge). Sulfurized polyacrylonitrile (SPAN) is one of the sulfur-based active materials, which allows more freedom in the Li–S cell design because it shows no undesirable reactions with electrolyte solutions. An original Li–S pouch cell construction (ADEKA's Lithium–Sulfur/Pouch Cell : ALIS-PC), the world's lightest rechargeable battery cell was designed by combining the SPAN cathode and state-of-the-art technologies. As a result, the highest gravimetric energy densities of 713 and 761 Wh/kg-cell after some charge-and-discharge cycles, which were based on the total mass of all cell components, were achieved with successful operating at 0.1 and 0.05C-rates, respectively, which significantly exceeded those of commercial lithium-ion and developed next-generation rechargeable batteries.

Lithium–sulfur (Li–S) rechargeable batteries, which are composed of sulfur-based cathodes, liquid electrolytes, and lithium–metal anodes, have been actively investigated as extremely promising next-generation energy storage devices because of the low-temperature synthetic processes of cathode active materials and Co- and Ni-free systems and the high gravimetric energy density at the single-cell level (Wh/kg-cell)[1–8]. For Li–S single cells, energy densities of over 500 Wh/kg-cell under low-rate conditions have been reported to date, with 695 Wh/kg-cell for pouch type being the highest value, which, however, could be attained only under conditions of a first discharge at an ultralow rate of 0.005C[9]. The realization of ultra-lightweight rechargeable batteries with stable operations will in turn lead to the realization of energy-efficient electric vehicles (EVs) and mobile

scooters, energy storage systems and battery stations, portable battery packs, drones, electric vertical take-off and landing (eVTOL) and high-altitude long-endurance (HALE) aircrafts, high-altitude platform stations (HAPSs), and others. The improved performance and commercialization of Li–S batteries will enrich our lives with EV revolution and urban air mobility (UAM)[10–12].

Sulfurized polyacrylonitrile (SPAN) is one of the sulfur-based active materials receiving the most attention, and numerous papers on this material have been reported since 2002. The following features of SPAN have attracted the attention of researchers[13–20]. It has a Co- and Ni-free chemical structure consisting of ubiquitous elements, S–C covalent bonds, and polymeric backbones of cyclized PAN (Supplementary Fig. 1). It is amenable to simple process and low-temperature synthetic process under 500 ºC, and has a moderate specific capacity of over 500 mAh/g (Supplementary Fig. 2). It shows better power performance than conventional sulfur-based active materials, and various electrolytes from liquids to solids without polysulfide shuttling are available (Supplementary Fig. 3). It possesses superior adsorption abilities of lithium polysulfides (Supplementary Fig. 4). It has no μL-electrolyte/mg-sulfur (E/S) ratio restrictions and it shows outstanding reversibility with almost 100% coulombic efficiency and over 500 cycles in charge-and-discharge (chg./dischg.) operations (Supplementary Fig. 5). Although these characteristics provide greater flexibility in Li–S cell design, the gravimetric energy densities of Li–SPAN cells have been limited to less than 500 Wh/kg-cell. In this work, an original Li–S pouch cell design, that is, ADEKA's Lithium–Sulfur/Pouch Cell (ALIS-PC), was realized by applying SPAN (ADEKA AMERANSA SAM-8) and ten state-of-the-art technologies. As a result, an 11 Ah ultra-lightweight Li–SPAN pouch cell with the energy densities of 713 and 761 Wh/kg-cell at 0.1 and 0.05C-rates at 30 ºC, respectively, after some chg./dischg. cycles was realized. These are the world record cell energy densities significantly exceeding those of commercial lithium-ion rechargeable batteries (LIBs) and new-type next-generation batteries under development such as lithium–metal batteries (LMBs) and lithium–air batteries (LABs) (Fig. 1 and Supplementary Table 1)[21–26].

Technology I. A 3D-Al foam sheet, Al-CELMET, was chosen as the current collector to increase the areal mass loading of sulfur in the SPAN cathode[27]. Figs. 2a and 2b respectively show a scanning electron microscopy (SEM) image of the SPAN cathode on the 3D-Al foam and the areal cathode capacities (mAh/cm^2) on the 3D-Al foam or conventional carbon-coated Al foil. A higher sulfur loading of 32.4 mg-S/cm^2 (68.0 mg-SPAN/cm^2) on both sides was achieved by stabilizing the thick SPAN layer in the 3D-Al foam, and four times the areal capacity of 46.6 mAh/cm^2 with a specific capacity of 686 mAh/g-SPAN (1441 mAh/g-S) and 100% coulombic efficiency at 0.1C-rate and 30 ºC was obtained reversibly. A superior performance of 770 mAh/g-SPAN was observed under the 0.01C-rate condition.

Technology II. The weight of 3D-Al foam with 96% porosity is 10 mg/cm^2; furthermore, a 31%

weight saving was achieved by a laser-drilling technique (Fig. 2c)[28]. On the other hand, further processing was not possible in terms of strength (Supplementary Fig. 6). Capacity losses due to processing was not seen at lower chg./dischg. rates despite the weight-saving processing, which reduced the current collection ability (Supplementary Fig. 7).

Technology III. The active material weight ratio in the cathode layer is also important for energy density improvement[2]. Single-walled carbon nanotube (SWCNT) conducting agents and cellulose nanofiber (CNF) binders, which can be added in small quantities because of their superior electrical conductivity with high surface area and mechanical strength with the thixotropic property in water, are highly useful materials for this purpose[29,30]. A cathode fabricated using these materials with a 98.0 wt% SPAN ratio was designed, and it showed a favorable specific capacity (Table 1).

Technology IV. SWCNTs are difficult to disperse owing to their strong cohesion, and as a result, ion diffusion in electrodes may deteriorate, instead of excellent electronic conductivity. A soft dispersing method, which disperses SWCNTs of good quality but does not cause damage, was selected, and Nihon Spindle Manufacturing's JET PASTER (JP) technique[31] was applied to SWCNT dispersion in H_2O. The SPAN cathode with the JP-treated SWCNT was found to have a low ohmic resistance (R_{ohm}) in the electrode (Supplementary Fig. 8).

Technology V. Compared with conventional lithium transition metal oxides and sulfur–carbon composites as the cathode active materials, polymer-based materials provide a higher degree of freedom in terms of shape design[32]. Mixing active materials of particle and fiber shapes would improve electronic and ionic conductivities in the electrode. At the optimum blend ratio (90/10) of SPAN particles and fibers, the electronic conductivity remained approximately the same, but the ion diffusion resistance (R_{ion}) was reduced specifically in the SPAN cathode (Figs. 3a, 3b, and Supplementary S9). This result was analyzed by 3D microstructure simulations for models of SPAN cathodes and found to be due to the low-tortuosity pores for the lithium-ion transport path in the cathode (Supplementary Fig. 10).

Technology VI. In the high-sulfur-loading thick cathodes demanded for superior energy densities, electrolyte solutions may be depleted during chg./dischg. cycle operations. To improve the performance of electrolyte retention in the thick electrodes, a porous SPAN fiber was effective (Figs. 3c, 3d, and Supplementary S11). The application of the porous SPAN fiber with excellent electrolyte solution absorbency was also effective in the cell assembly process (Supplementary Fig. S12).

Technology VII. The chg./dischg. operation potential range of SPAN cathodes is limited within 3.0–1.0 V (*vs.* Li/Li^{+}) to utilize the sulfur redox reaction[13–20]. On the other hand, the cyclized-PAN backbone was electrochemically active[33] and had reversible capacities at the lower potentials (<1.0 V). An expanded chg./dischg. operation was performed in a potential range of 3.5–0.3 V to prevent undesirable side reactions of the Al current collector and carbonate/ether electrolyte solutions[34,35]. As a result, higher specific capacities of 1006 mAh/g-SPAN (2113 mAh/g-S) with 100% coulombic

efficiency at 0.1C-rate and 1102 mAh/g-SPAN (2315 mAh/g-S) at 0.05C-rate were observed after ten cycles at 30 ºC (Fig. 4).

Technology VIII. In general, 30–60% of the Li–S pouch cell weight is attributable to the electrolyte solutions; therefore, reducing the weight of the solutions is essential for improving the gravimetric energy density[2,6,9,36–38]. A new ether-based electrolyte solution (Light-Ele) with the combined properties of light weight (0.98 g/cm^3), high ionic conductivity, and low viscosity was developed and confirmed to work in the Li–SPAN cell (Supplementary Table 2 and Supplementary Fig. 13). However, the activity of SPAN with the Light-Ele was lower than those with the conventional carbonate-based electrolyte solutions, and we inferred that the quality of a cathode–electrolyte–interphase (CEI) film was poor in the case of the Light-Ele. Our idea to solve this problem is to apply a two-step chg./dischg. method using two different electrolytes. In the first step, a carbonate-based electrolyte solution with FEC and LiBOB additives is used to form a suitable CEI film[39,40], and in the second step, ether-based Light-Ele is used to reduce cell weight after removing the electrolyte used in the first step. The two-step method was successfully applied, resulting in sufficient SPAN performance in Light-Ele (Table 2). This new technique is unique to SPAN, which can operate with a variety of electrolyte solutions. Furthermore, SPAN can reduce the amount of electrolyte solutions in the cells because the elution of sulfur components into electrolyte solutions hardly occurs, and this two-step method enabled further reductions.

Technology IX. A thinner separator is also essential for increasing the cell energy density, but Li–S cells are prone to short circuits when a thin separator is used. The SETELA PE-type separator film, which is 5 μm thick and has 35% porosity favorable for lightweight cells, showed a good affinity for Li–SPAN cells (Supplementary Table 3). In addition, a thinner pouch of an aluminum laminated film with a thickness under 80 μm (thin-type DNP Battery Pouch) was also applied.

Technology X. To maximize the energy density performance of Li–metal anode cells, anode-free configuration designs, that is, lithium deposits on the bare current collector without any host materials, are useful, and there have been many reports on cells with Li-containing cathode active materials[41–46]. Since SPAN does not contain the Li element, an electrochemical prelithiation strategy using the half-cell method was applied to the SPAN cathode. The carbonate-based electrolyte solution with FEC and LiBOB additives was used for the prelithiation and the ether-based Light-Ele for the completed cell with the lithiated SPAN cathode and the anode-free configuration design. In other words, the two-step chg./dischg. method with two different electrolyte solutions described above was well applied to the anode-free-type Li–SPAN cell. The low coulombic efficiency and Li-dendrite deposition straiten a stable cell operation in the anode-free designs. We solved the problems by applying an ultra-thin Li foil of ca. 10 μm thickness as the negative current collector instead of the conventional Cu foil and also by using the electrolyte additive LiHFDF[47] in the Light-Ele. The 100% coulombic efficiency allowed for a reduction in the amount of electrolyte

solution, and SPAN is not limited by the E/S ratio unlike other sulfur-based active materials[11,12,48,49]. In addition, lithium has a significantly lower density (0.53 g/cm^3) than copper (8.96 g/cm^3); therefore, this design has an ideal material choice for ultra-lightweight cells. Fig. 5 shows an original Li–S pouch cell design that consolidates the state-of-the-art technologies described above, which is named ALIS-PC (ADEKA's Lithium–Sulfur/Pouch Cell). SPAN is probably the most suitable cathode active material for the ALIS-PC design.

Ultra-lightweight cell.   An ultra-lightweight Li–SPAN pouch cell with the ALIS-PC design realized by applying the above ten technologies was assembled with an 11 Ah-class capacity. Fig. 6 and Supplementary Fig. 14 show chg./dischg. cycle performance and characteristic curves in five cycles at 0.1C-rate and 30 ºC. An outstanding discharge performance at 11.31 Ah and 1.64 V was observed in the 26.03 g-cell (without fixtures), and the gravimetric energy density was calculated to be 713 Wh/kg-cell (volumetric; 832 Wh/L-cell). At a lower rate operation of 0.05C, the energy densities were 761 Wh/kg-cell (12.01 Ah and 1.65 V) and 800 Wh/kg excluding the weights of the pouch film and metal tabs.

In conclusion, by fabricating the world's lightest rechargeable battery cell with >750 Wh/kg-cell (Supplementary Fig. S15), we clearly demonstrated the potential of Li–SPAN designs to approach innovative post-LIB realizations (Fig. 1 and Supplementary Table 1). Recently, a wide variety of rechargeable batteries have been in demand, and this study can provide some of the most important results to meet the demand. We envision a future in which the commercialization and practical application of Li–SPAN batteries will exploit new markets and accelerate the development of a sustainable and prosperous society.

Methods

Preparation of SPAN cathodes: The aqueous slurries for the cathode layer coating were prepared by mixing sulfurized polyacrylonitrile particle [SPAN: ADEKA AMERANSA SAM-8 / 48 wt% sulfur content / D_{50} = 3 μm / particle density = 1.9 g/cm^3; ADEKA Corporation (Supplementary Fig. 16)] as the active material with acetylene black (AB; DENKA BLACK Li-100, Denka Company Limited), multi-walled carbon nanotube (MWCNT; FT9000, Jiangsu Cnano Technology Co., Ltd.), or single-walled carbon nanotube (SWCNT; Lamfil WPB-043 / H$_2$O dispersion, Kusumoto Chemicals, Ltd.) as conductive agents and styrene–butadiene rubber (SBR; BM-451B / water-based, Zeon Corporation) and sodium carboxymethyl cellulose (CMC-Na; CELLOGEN BSH-6, DKS Co., Ltd. or DAICEL CMC 2200, Daicel Miraizu Ltd.) and cellulose nanofiber (CNF; under development, ADEKA Corporation) as binders at SPAN:AB:SBR:CMC-Na weight ratios of 92.0/5.0/1.5/1.5,

94.0/3.0/1.5/1.5, and 96.0/1.0/1.5/1.5; or SPAN:MWCNT:SBR:CMC-Na weight ratio of 97.4/1.0/0.7/0.9; or SPAN:SWCNT:SBR:CMC-Na weight ratios of 97.4/1.0/0.7/0.9, 97.7/0.7/0.7/0.9, and 98.0/0.4/0.7/0.9; or SPAN:SWCNT:SBR:CMC-Na:CNF weight ratio of 98.0/0.4/0.7/0.7/0.2. The dispersion of SWCNT in H_2O using the JET PASTER JPSS-X was carried out by Nihon Spindle Manufacturing Co., Ltd. SPAN fiber and porous fiber with ca. 500 nm diameter were synthesized as follows. 10 wt% polyacrylonitrile (PAN) and PAN/poly(methyl methacrylate) (90/10 by weight, Merck KGaA) solutions were used as spinning solutions. A predetermined amount of polymer powder was dissolved in N,N-dimethylformamide (99.5%, Nacalai Tesque Inc.) by stirring at room temperature (RT) for 2 h and then at 60 °C for 6 h, which was followed by slow cooling to RT. The prepared solution was electrospun using a NEU Nanofiber Electrospinning Unit (KATO TECH CO., LTD.). The voltage and flow rate were fixed at 15 kV and 1.0 mL/h, respectively. The inner diameter of the nozzle (stainless-steel needle) and the distance between the needle tip and the rotating collector were 0.94 mm and 100 mm, respectively. The collector, which was covered with aluminum foil, was rotated at a speed of 1 m/min. The temperature and ambient humidity throughout the process were 25 °C and 25%, respectively. The obtained electrospun polymer fibers were peeled off from the aluminum foil. The polymer fibers and excess elemental sulfur (S_8, Hosoi Chemical Industry Co., Ltd.) were mixed by using a mortar and pestle, and the mixtures were maintained at 300–500 °C in a nitrogen atmosphere for thermal conversion reactions. Subsequent heat treatments removed the elemental sulfur, which was confirmed by powder XRD analyses (Supplementary Fig. 17) using Cu-Kα radiation at 40 kV and 40 mA (Ultima IV, Rigaku Corporation). An elemental analysis confirmed a sulfur content of 48 wt% in the SPAN fibers, and the fibers became porous when using PAN/poly(methyl methacrylate) as the raw material. Portions of the SPAN particle (SAM-8) in the cathodes were replaced by the SPAN fibers. Subsequently, the obtained aqueous SPAN slurries were coated onto carbon-coated aluminum (Al) foil (SDX, Showa Denko K.K.) or 3D-Al foam sheet (Al-CELMET, 1.0 mm thick / 96% porosity /10 mg/cm^2, Sumitomo Electric Industries, Ltd.) as cathode current collectors and dried in ovens at 80 °C for 8 h or 70 °C for 15 h, respectively. The laser drilling of the 3D-Al foam for weight saving was carried out by WIRED Co., Ltd. The SPAN electrode with the weight saved 3D-Al foam possessing a thickness of 578 μm, a SPAN loading of 68.0 mg/cm^2, a density of 1.2 g/cm^3, and 36% porosity was obtained using roll press equipment (Oono-roll Corporation). Lastly, the cathodes were shaped into 12-φ disc-size for coin-type cells or 8.0×4.2 cm^2 rectangle-size for pouch-type cells, and dried in a vacuum oven at 130 °C for 15 h before cell assembling.

Preparation of electrolyte solutions: 1.0 M $LiPF_6$ in EC/DEC (50/50, vol%), 1.0 M $LiPF_6$ in FEC/DEC (50/50, vol%), 1.0 M $LiPF_6$ in FEC/DEC (50/50, vol%) + 2 wt% LiBOB, 1.0 M LiTFSI in DOL/DME (50/50, vol%) + 2 wt% $LiNO_3$, 0.4 M LiTFSI + 0.4 M $LiNO_3$ + 0.1 M LiHFDF in DME/DOL/TFMTMS (48/17/35, vol%)[38], and Light-Ele of 0.2 M LiTFSI + 0.2 M LiFSI + 0.1 M

LiNO$_3$ + 0.1 M LiHFDF in DME/DOL/TFMTMS (75/5/20, vol%) were prepared in an Ar-filled glove box. The water contents in the solutions were controlled to be under 30 ppm. Electrolyte solutions of 1.0 M LiPF$_6$ in EC/DEC (50/50, vol%) and 1.0 M LiPF$_6$ in FEC/DEC (50/50, vol%) were purchased from KISHIDA CHEMICAL CO.,LTD. Lithium bis(fluorosulfonyl)imide LiN(SO$_2$F)$_2$ (LiFSI; IONEL LF-101) was provided by NIPPON SHOKUBAI CO., LTD. Lithium nitrate (LiNO$_3$) was purchased from FUJIFILM Wako Pure Chemical Corporation, and other materials such as lithium bis(oxalate)borate (LiBOB), 1,3-dioxolane (DOL), 1,2-dimethoxyethane (DME), lithium 1,1,2,2,3,3-hexafluoropropane-1,3-disulfonimide (LiHFDF), (trifluoromethyl)trimethylsilane (TFMTMS), and lithium bis(trifluoromethanesulfonyl)imide (LiTFSI) were purchased from Tokyo Chemical Industry Co., Ltd.

Cell assemblies: Coin-type and pouch-type cells were assembled in dry spaces with dew points between -50 and -75 °C using a Dry Room System (Seibu Giken Co., Ltd.) and a NS DRY BOOTH (Nihon Spindle Manufacturing Co., Ltd.). The compositions of 2032 coin-type cells were as follows: SPAN cathodes (12φ) | Celgard 2325 and ADVANTEC GA-100 separators (16φ) | Li–metal anode without Cu foil (14φ / 500 μm thick, Honjo Metal Co., Ltd.) with filled electrolyte solutions. The coin-cell pieces were purchased from Hohsen Corp. In the case of ultra-lightweight pouch-type cells, 5 sheets of the SPAN cathodes with the 3D-Al foam (8.0×4.2 cm^2), 10 sheets of a SETELA-05C separator (8.4×4.6 cm^2 / PE / 5 μm thick / 35% porosity, Toray Industries, Inc.), and 6 sheets of a Li–metal anode current collector without Cu foil (8.7×4.4 cm^2 / ca. 10 μm thick, Honjo Chemical Corporation) were alternately stacked, and then an Al tab for the cathode, a Ni-tab for the anode, and Al-laminated film (DNP Battery Pouch / D-EL30H(3)20 / 77 μm / 0.013g/cm^2, Dai Nippon Printing Co., Ltd.) were attached to the stacked electrodes. After electrolyte injection, the pouch cells were heat-sealed and ready for battery operations. The E/S ratio in the case of the Light-Ele was 1.4 μL/mg. A 500-μm-thick Li–metal anode with a Cu foil (10 μm thick) and excess carbonate electrolyte solutions in large amounts were used for the electrochemical prelithiation of the SPAN cathodes for five cycles at 0.1C-rate and 30 ºC, and the prelithiated cathodes were washed by using dehydrated dimethyl carbonate. All pouch-type cells were strongly constrained with fixtures in chg./dischg. operations.

Cell operations and analyses: Charge-and-discharge (chg./dischg.) measurements were performed by using the chg./dischg. test systems TOSCAT (TOYO SYSTEM CO., LTD.) and BLS (KEISOKUKI CENTER CO., LTD.) at 30 °C. The cut-off voltages of 3.0/1.0, 3.0/0.3, 3.5/1.0, and 3.5/0.3 V were set for chg./dischg. steps. CCCV-chg. (CV time = 30 min.)/CC-dischg. and CC-chg./CC-dischg. modes were used in 11 Ah-class pouch cells and other cells, respectively. Electrochemical impedance spectroscopy (EIS) measurements using Solartron 1286 Potentiostat/Electrochemical Interface and Solartron 1260 Impedance/Gain-Phase Analyzer (AMETEK, Inc. / Solartron Analytical) were carried out in the frequency range from 100 kHz to 0.1

Hz with a sinusoidal AC voltage amplitude of 10 mV. The EIS data were analyzed by using the ZView software program. Regulus8220 (Hitachi High-Tech Corporation), Ultim Max 100 (Oxford Instruments KK), and Ultramicrotome Leica EM UC7 (Leica Microsystems GmbH) were used for field emission scanning electron microscope (FE-SEM) observation and energy-dispersive X-ray spectroscopy (EDX) elemental mapping. Tortuosity simulations of the SPAN electrode models with/without the SPAN fiber were performed using the GeoDict software (Math2Market GmbH)[50], and calculations were carried out by NISSAN ARC, LTD.

References

1. Shao, Q., Zhu, S. & Chen, J. A review on lithium−sulfur batteries: challenge, development, and perspective. *Nano Res.* **16**, 8097–8138 (2023).

2. Zhou, G., Chen, H. & Cui, Y. Formulating energy density for designing practical lithium–sulfur batteries. *Nat. Energy* **7**, 312−319 (2022).

3. Chen, Z.-X., Zhao, M., Hou, L.-P., Zhang, X.-Q., Li, B.-Q. & Huang, J.-Q. Toward practical high-energy-density lithium–sulfur pouch cells: a review. *Adv. Mater.* **34**, 2201555 (2022).

4. Wang, M., Bai, Z., Yang, T., Nie, C., Xu, X., Wang, Y., Yang, J., Dou, S. & Wang, N. Advances in high sulfur loading cathodes for practical lithium−sulfur batteries. *Adv. Energy Mater.* **12**, 2201585 (2022).

5. Tan, J., Yao, Z., Ye, M. & Shen, J. An optimized combination inspired by the wooden-barrel effect for Li–S pouch cells. *Cell Rep. Phys. Sci.* **2**, 100659 (2021).

6. Robinson, J. B. et al. 2021 roadmap on lithium sulfur batteries. *J. Phys. Energy* **3**, 031501 (2021).

7. Zhao, M., Li, B.-Q., Zhang, X.-Q., Huang, J.-Q. & Zhang, Q. A perspective toward practical lithium−Sulfur Batteries. *ACS Cent. Sci.* **6**, 1095−1104 (2020).

8. Manthiram, A., Fu, Y., Chung, S.-H., Zu, C. & Su, Y.-S. Rechargeable lithium–sulfur batteries. *Chem. Rev.* **114**, 11751−11787 (2014).

9. Cheng, Q., Chen, Z.-X., Li, X.-Y., Hou, L.-P., Bi, C.-X., Zhang, X.-Q., Huang, J.-Q. & Li, B.-Q. Constructing a 700 Wh kg^{-1}-level rechargeable lithium−sulfur pouch cell. *J. Energy Chem.* **76**, 181−186 (2023).

10. Dörfler, S., Walus, S., Locke, J., Fotouhi, A., Auger, D. J., Shateri, N., Abendroth, T., Härtel, P., Althues, H. & Kaskel, S. Recent progress and emerging application areas for lithium–sulfur battery technology. *Energy Technol.* **9**, 2000694 (2021).

11. Wird, M. & Offer, G. J. (Eds.) *Lithium–Sulfur Batteries* (Wiley, 2019).

12. Demir-cakan, R. (Ed.) *Li-S Batteries: The Challenges, Chemistry, Materials and Future Perspectives* (World Scientific Publishing, 2017).

13. Zhang, X., Ma, H., Liu, J., Chen, J., Lu, H., Huang, Y. & Wang, J. *Nano Res.* **16**, 8159–8172 (2023).

14. Huang, J., Shao, Y., Liu, Z., Lv, Y., Guo, F., Tu, Y., Ichikawa, T., Hu, Z. & Zhang, T. Nano sulfurized polyacrylonitrile cathode for high performance solid-state lithium–sulfur batteries. *Journal of Power Sources* **570**, 233045 (2023).

15. Ahmed, M. S., Lee, S., Agostini, M., Jeong, M.-G., Jung, H.-G., Ming, J., Sun, Y.-K., Kim, J., & Hwang, J.-Y. Multiscale understanding of covalently fixed sulfur–polyacrylonitrile composite as advanced cathode for metal–sulfur batteries. *Adv. Sci.* **8**, 2101123 (2021).

16. Zhao, X., Wang, C., Li, Z., Hu, X., Razzaq, A. A. & Deng, Z. Sulfurized polyacrylonitrile for high-performance lithium sulfur batteries: advances and prospects. *J. Mater. Chem. A* **9**, 19282−19297 (2021).

17. Chen, W.-J., Li, B.-Q., Zhao, C.-X., Zhao, M., Yuan, T.-Q., Sun, R.-C., Huang, J.-Q. & Zhang, Q. Electrolyte regulation towards stable lithium-metal anodes in lithium–sulfur batteries with sulfurized polyacrylonitrile cathodes. *Angew. Chem. Int. Ed.* **59**, 10732–10745 (2020).

18. Chen, X., Peng, L., Wang, L., Yang, J., Hao, Z., Xiang, J., Yuan, K., Huang, Y., Shan, B., Yuan, L. & Xie, J. Ether-compatible sulfurized polyacrylonitrile cathode with excellent performance enabled by fast kinetics via selenium doping. *Nat. Commun.* **10**, 1021 (2019).

19. Zhang, S. S. Understanding of sulfurized polyacrylonitrile for superior performance lithium/sulfur battery. *Energies* **7**, 4588−4600 (2014).

20. Wang, J., Yang, J., Xie, J. & Xu, N. A novel conductive polymer–sulfur composite cathode material for rechargeable lithium batteries. *Adv. Mater.* **14**, 963−965 (2002).

21. Edström, K. et al. *BATTERY 2030+ Roadmap* Fig. 9 https://battery2030.eu/wp-content/uploads/2022/07/BATTERY-2030-Roadmap_Revision_FINAL.pdf (2022).

22. Houache, M. S. E., Yim, C.-H., Karkar Z. & Abu-Lebdeh, Y. On the current and future outlook of battery chemistries for electric vehicles—mini review. *Batteries* **8**, 70 (2022).

23. Wu, F., Fang, S., Kuenzel, M., Mullaliu, A., Kim, J.-K., Gao, X., Diemant, T., Kim, G.-T. & Passerini, S. Dual-anion ionic liquid electrolyte enables stable Ni-rich cathodes in lithium-metal

batteries. *Joule* **5**, 2177−2194 (2021).

24. Enpower Greentech Inc. & Enpower Japan Corp. *Press Release (Enpower Successfully Develops a Record-Breaking Lithium Metal Battery)* https://enpowerjp.co.jp/wp-content/uploads/2021/10/Enpower-News-Release-2021-10-25_English.pdf (2021).

25. SoftBank Corp. & HAPSMobile Inc. *Press Release (SoftBank Corp. Develops Battery Pack with Next-generation Lithium-metal Battery Cells and Successfully Demonstrates Operation in the Stratosphere)* https://www.softbank.jp/en/corp/news/press/sbkk/2023/20230316_01/ (2023).

26. Matsuda, S., Ono, M., Yamaguch, S. & Uosaki, K. Criteria for evaluating lithium–air batteries in academia to correctly predict their practical performance in industry. *Mater. Horiz.* **9**, 856–863 (2022).

27. Matsumae, Y., Obata, K., Ando, A., Yanagi, M., Kamei, Y., Ueno, K., Dokko, K. & Watanabe, M. Effects of sulfur loading, cathode porosity, and electrolyte amount on Li–S battery performance with solvate ionic liquid electrolyte. *Electrochemistry* **87**, 254–259 (2019).

28. Tsuda, T., Ando, N., Nakamura, S., Ishihara, Y., Hayashi, N., Soma, N., Gunji, T., Tanabe, T., Ohsaka, T. & Matsumoto, F. Improvement of high-rate discharging performance of $LiFePO_4$ cathodes by forming micrometer-sized through-holed electrode structures with a pico-second pulsed laser. *Electrochim. Acta* **296**, 27–38 (2019).

29. Predtechenskiy, M. R. et al. New perspectives in SWCNT applications: Tuball SWCNTs. part 2. new composite materials through augmentation with Tuball. *Carbon Trends* **8**, 100176 (2022).

30. Cao, S., Feng, X., Song, Y., Xue, X., Liu, H., Miao, M., Fang, J. & Shi, L. Integrated fast assembly of free-standing lithium titanate/carbon nanotube/cellulose nanofiber hybrid network film as flexible paper-electrode for lithium-ion batteries. *ACS Appl. Mater. Interfaces* **7**, 10695–10701 (2015).

31. Kimura, K., Sakamoto, T., Mukai, T., Ikeuchi, Y., Yamashita, N., Onishi, K., Asami, K. & Yanagida, M. Improvement of the cyclability and coulombic efficiency of Li-ion batteries using $Li[Ni_{0.8}Co_{0.15}Al_{0.05}]O_2$ cathode containing an aqueous binder with pressurized CO_2 gas treatment. *J. Electrochem. Soc.* **165**, A16–A20 (2018).

32. Wu, Q., Zhang, W., Li, S., Zhong, W., Zhu, H., Zeng, Z., Yu, C., Cheng, S. & Xie, J. Electrospun sulfurized polyacrylonitrile nanofibers for long-term cycling stability and high-rate lithium–sulfur batteries. *ACS Appl. Energy Mater.* **5**, 5212−5218 (2022).

33. Liu, Q., Xiao, Z., Cui, X., Deng, S., He, Q., Zhang, Q., Lin, Z. & Yang, Y. Conjugated cyclized-polyacrylonitrile encapsulated carbon nanotubes as core–sheath heterostructured anodes with favorable lithium storage. *J. Mater. Chem. A* **9**, 6962–6970 (2021).

34. Li, H., Yamaguchi, T., Matsumoto, S., Hoshikawa, H., Kumagai, T., Okamoto, N. L. & Ichitsubo, T. Circumventing huge volume strain in alloy anodes of lithium batteries. *Nat. Commun.* **11**, 1584 (2020).

35. Matsumoto, K., Inoue, K., Nakahara, K., Yuge, R., Noguchi, T. & Utsugi, K. Suppression of aluminum corrosion by using high concentration LiTFSI electrolyte. *J. Power Sources* **231**, 234–238 (2013).

36. Kang, N., Lin, Y., Yang, L., Lu, D., Xiao, J., Qi, Y. & Cai, M. Cathode porosity is a missing key parameter to optimize lithium-sulfur battery energy density. *Nat. Commun.* **10**, 4597 (2019).

37. Liu, T., Li, H., Yue, J., Feng, J., Mao, M., Zhu, X., Hu, Y., Li, H., Huang, X., Chen, L. & Suo, L. Ultralight electrolyte for high-energy lithium–sulfur pouch cells. *Angew. Chem. Int. Ed.* **60**, 17547–17555 (2021).

38. Liu, T., Shi, Z., Li, H., Xue, W., Liu, S., Yue, J., Mao, M., Hu, Y., Li, H., Huang, X., Chen, L. & Suo, L. Low-density fluorinated silane solvent enhancing deep cycle lithium–sulfur batteries' lifetime. *Adv. Mater.* **33**, 2102034 (2021).

39. Yang, H., Naveed, A., Li, Q., Guo, C., Chen, J., Lei, J., Yang, J., Nuli, Y. & Wang, J. Lithium sulfur batteries with compatible electrolyte both for stable cathode and dendrite-free anode. *Energy Stor. Mater.* **15** 299–307 (2018).

40. Jin, F., Hu, C., Liu, C., Zheng, Y., Chen, H., Shen, Y. & Chen, L. Enhancing the performance of sulfurized polyacrylonitrile cathode by in-situ wrapping. *J. Electroanal. Chem.* **835** 156–160 (2019).

41. Jo, C.-H., Sohn, K.-S. & Myung, S.-T. Feasible approaches for anode-free lithium-metal batteries as next generation energy storage systems. *Energy Stor. Mater.* **57**, 471–496 (2023).

42. Liu, Y., Meng, X., Wang, Z. & Qiu, J. Development of quasi-solid-state anode-free high-energy lithium sulfide-based batteries. *Nat. Commun.* **13**, 4415 (2022).

43. Huang, W.-Z., Zhao, C.-Z., Wu, P., Yuan, H., Feng, W.-E., Liu, Z.-Y., Lu, Y., Sun, S., Fu, Z.-H., Hu, J.-K., Yang, S.-J., Huang, J.-Q. & Zhang, Q. Anode-free solid-state lithium batteries: a review. *Adv. Energy Mater.* **12**, 2201044 (2022).

44. Louli, A. J., Eldesoky, A., deGooyer, J., Coon, M., Aiken, C. P., Simunovic, Z., Metzger, M. & Dahn, J. R. Different positive electrodes for anode-free lithium metal cells. *J. Electrochem. Soc.* **169**, 040517 (2022).

45. Qiao, Y., Yang, H., Chang, Z., Deng, H., Li, X. & Zhou, H. A high-energy-density and long-life initial-anode-free lithium battery enabled by a Li_2O sacrificial agent. *Nature Energy* **6**, 653–662 (2021).

46. Kwon, H., Lee, J.-H., Roh, Y., Baek, J., Shin, D. J., Yoon, J. K., Ha, H. J., Kim, J. Y. & Kim, H.-T. *Nat. Commun.* **12**, 5537 (2021).

47. Xiao, Y., Han, B., Zeng, Y., Chi, S.-S., Zeng, X., Zheng, Z., Xu, K. & Deng, Y. New lithium salt forms interphases suppressing both Li dendrite and polysulfide shuttling. *Adv. Energy Mater.* **10**, 1903937 (2020).

48. Yoshie, Y., Hori, K., Mae, T. & Noda, S. High-energy-density Li–S battery with positive

electrode of lithium polysulfides held by carbon nanotube sponge. *Carbon* **182**, 32–41 (2021).

49. Guo, J., Pei, H., Dou, Y., Zhao, S., Shao, G. & Liu, J. Rational designs for lithium–sulfur batteries with low electrolyte/sulfur ratio. *Adv. Funct. Mater.* **31**, 2010499 (2021).

50. Nguyen, T.-T., Demortière, A., Fleutot, B., Delobel, B. Delacourt, C. & Cooper, S. J. The electrode tortuosity factor: why the conventional tortuosity factor is not well suited for quantifying transport in porous Li-ion battery electrodes and what to use instead. *NPJ Comput. Mater.* **6**, 123 (2020).
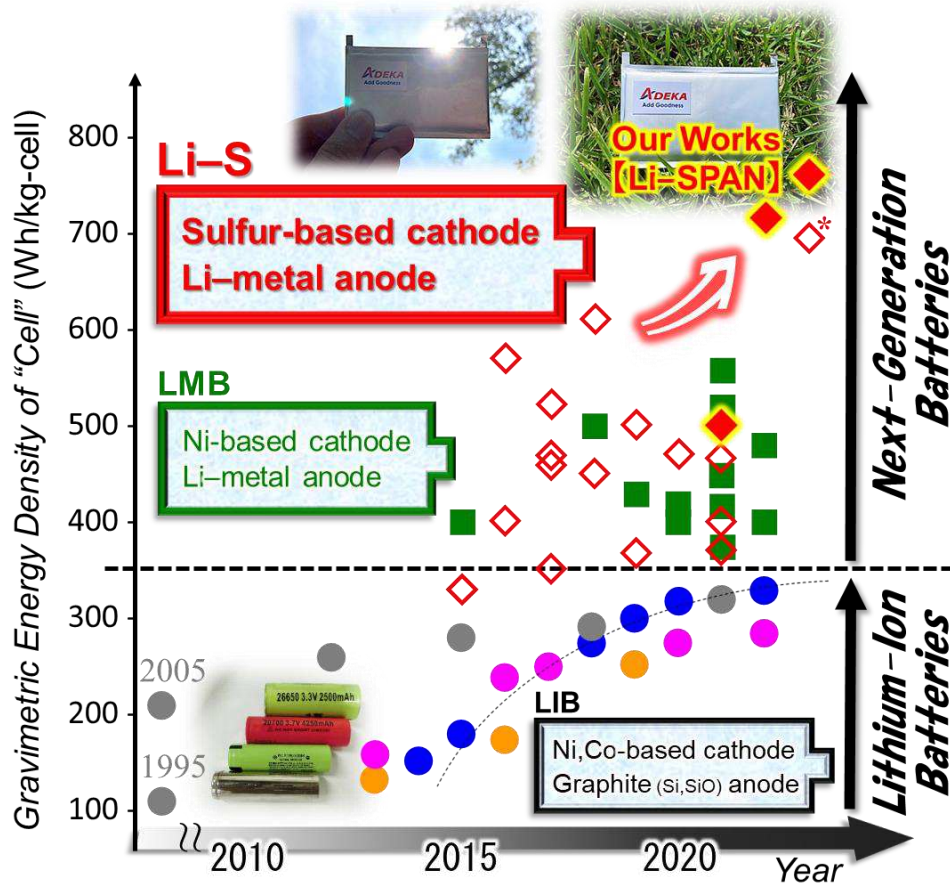
Fig. 1 | Gravimetric energy densities of various rechargeable battery cells for products, under developments, and researches. The data of LIBs are for Panasonic Energy Co., Ltd., LG Chem/LG Energy Solution Ltd., Samsung SDI Co.,Ltd., and Contemporary Amperex Technology Co., Limited. The data of next-generation batteries (Li–S batteries and LMBs) are for Enpower Japan Corp./Enpower Greentech Inc., SoftBank Corp., GS Yuasa Corporation, Sion Power Corporation, Cuberg, SES AI Corporation, and references[2,5,21−26]. An asterisk mark indicates an unstable chg./dischg. performance, the cell energy density is only in the first discharge[9].
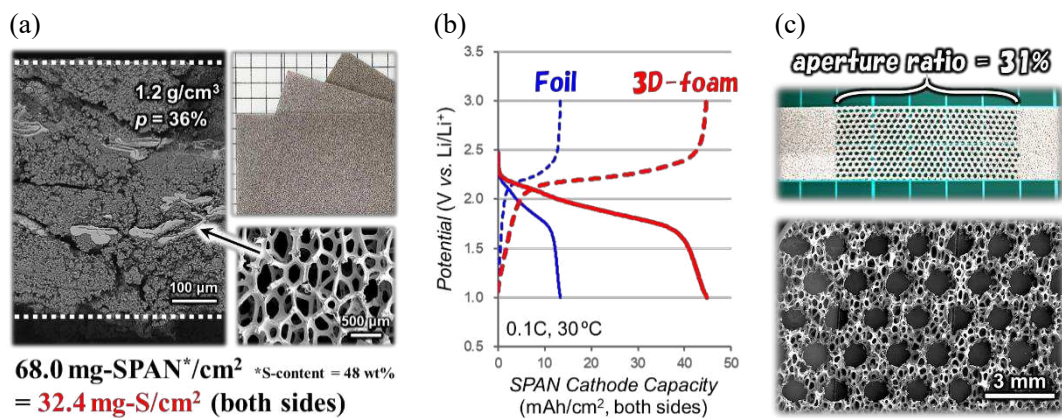
Fig. 2 | SPAN cathode and 3D-Al foam sheets as the current collector. a, Cross-sectional SEM image of the thick SPAN layer in the 3D-Al foam with a density of 1.2 g/cm^3 and a porosity of 36% and photographs of the 3D-Al foam (Al-CELMET). **b**, Reversible chg./dischg. properties at 0.1C-rate and 30 °C of the SPAN cathodes with carbon-coated Al foil or 3D-Al foam sheet in pouch cells (SPAN cathodes | carbonate electrolyte solution | Li–metal anode). **c**, Photographs of the porous 3D-Al foam sheet weight-saved by the laser-drilling technique.
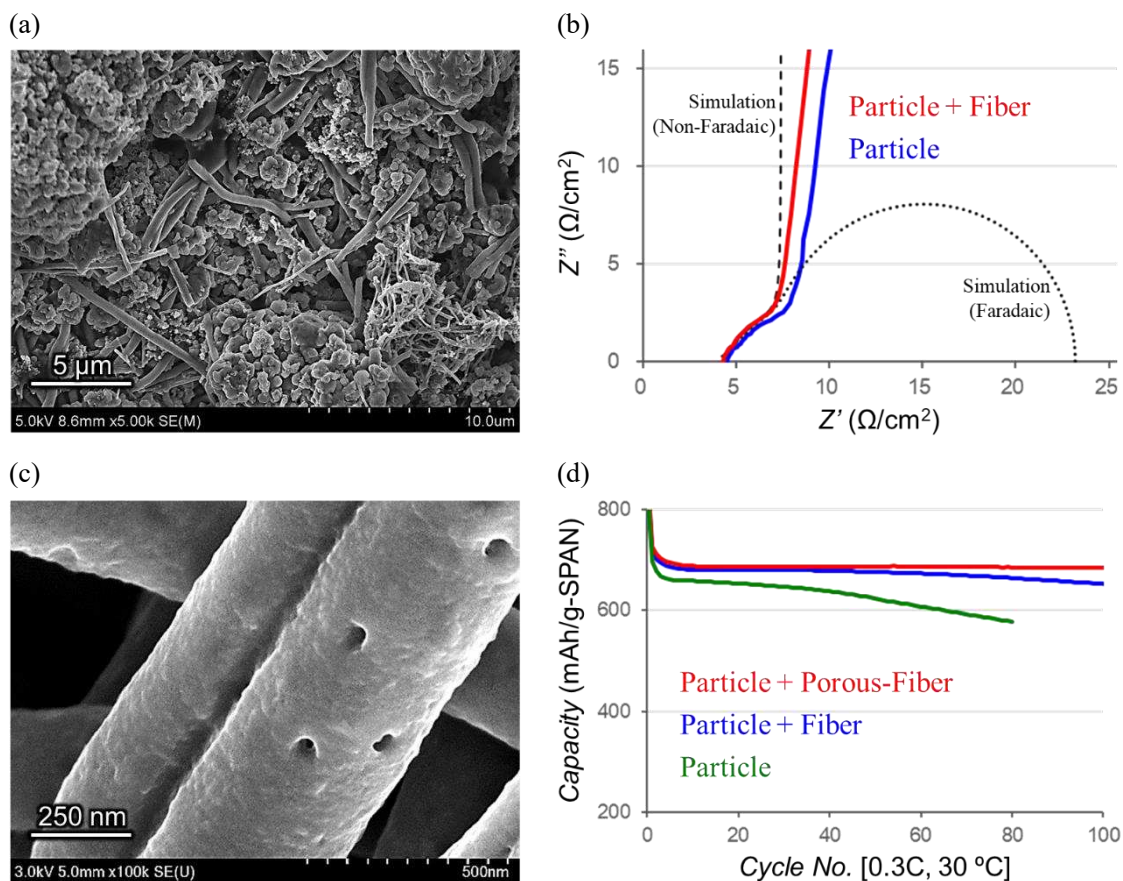
Fig. 3 | SPAN cathodes with fiber or porous fiber. a, SEM image of the SPAN cathode consisting of 90 wt% particle and 10 wt% fiber. **b**, Nyquist plots at 30 ºC of the SPAN cathodes with/without the SPAN fiber under a non-faradaic condition in symmetric coin cells (SPAN cathode | carbonate electrolyte solution with FEC | SPAN cathode). **c**, SEM image of the porous SPAN fiber. **d**, Chg./dischg. cycle performances at 0.3C-rate and 30 ºC of thick SPAN cathodes in the 3D-Al foam with/without the SPAN fibers in pouch cells (SPAN cathodes | carbonate electrolyte solution | Li–metal anode).
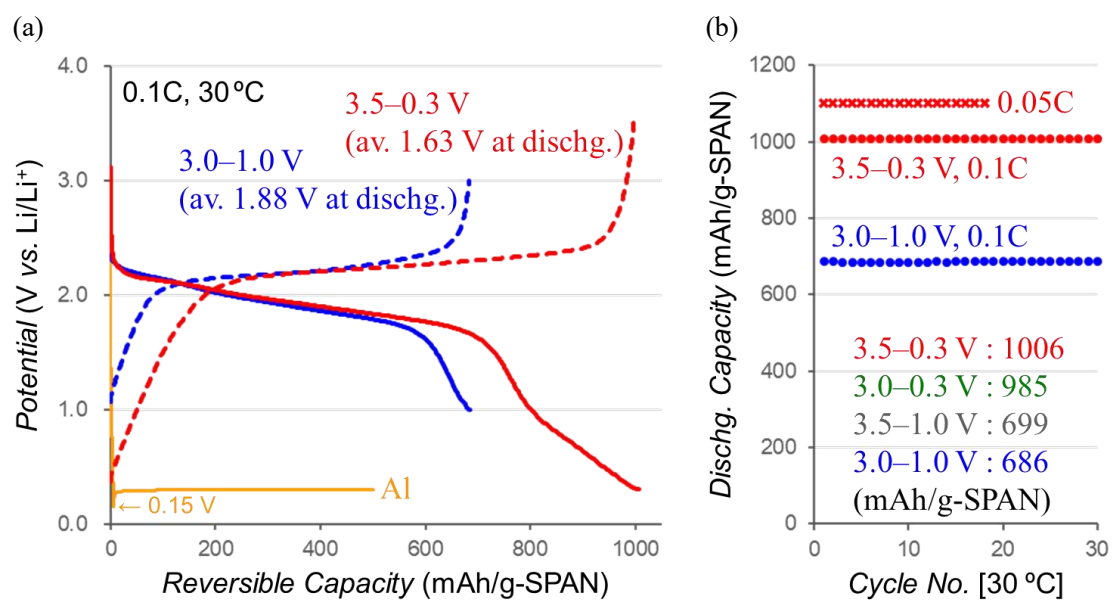
Fig. 4 | Chg./dischg. characteristics of the SPAN cathode with expanded operations in coin cells (SPAN cathode | carbonate electrolyte solution with FEC | Li–metal anode). a, Reversible chg./dischg. properties at 0.1C-rate and 30 ºC and a reaction potential between Al and Li. **b**, Chg./dischg. cycle performances at 0.1 and 0.05C-rates and 30 ºC after a formation process of ten cycles at 0.1C-rate and 30 ºC.
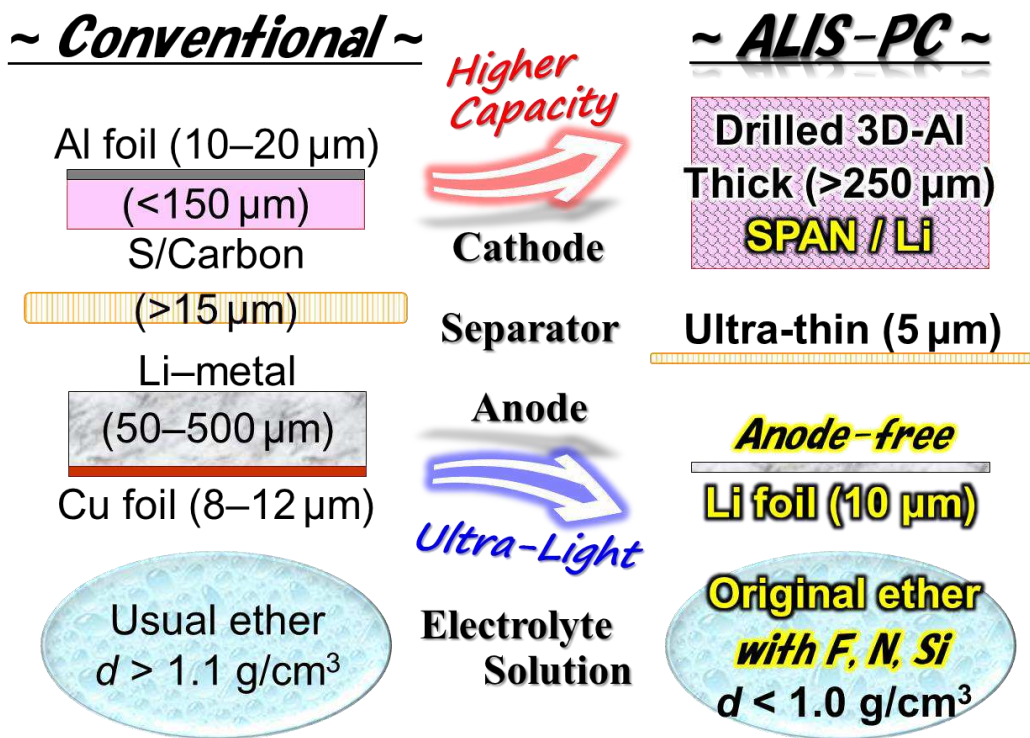
Fig. 5 | ALIS-PC design with the SPAN cathode for an ultra-lightweight Li–S rechargeable battery cell.
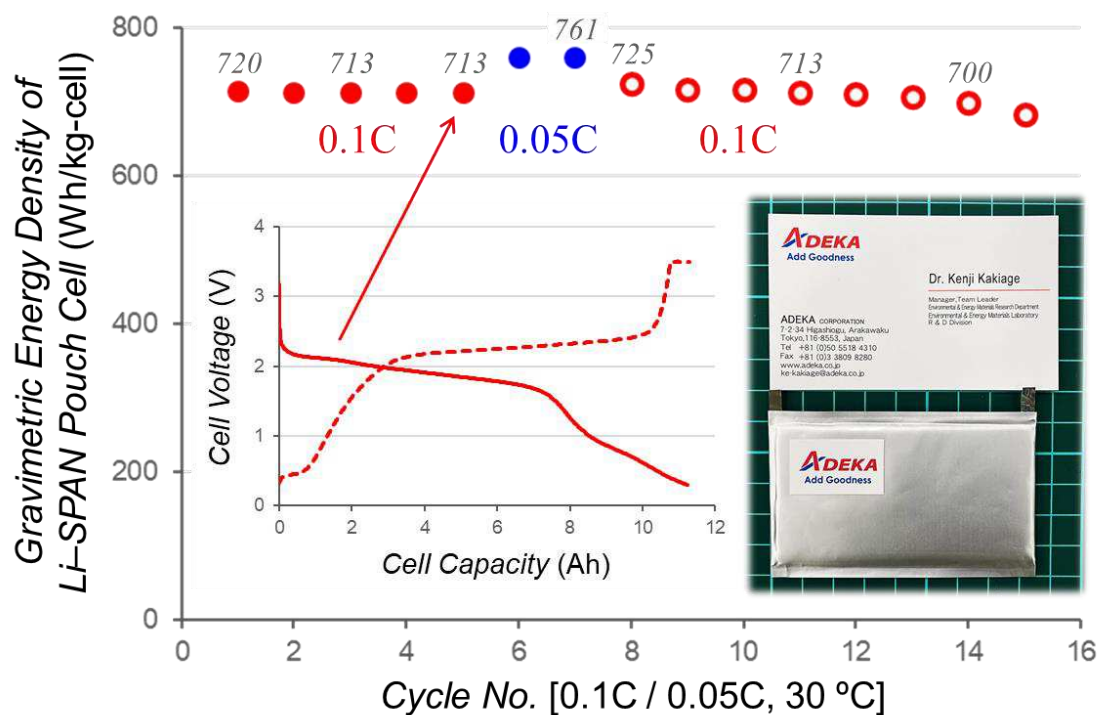
Fig. 6 | Chg./dischg. cycle performance of the ultra-lightweight Li–SPAN pouch cell with the ALIS-PC design. 0.1 and 0.05C-rates properties at 30 ºC, chg./dischg. characteristic curves at 0.1C-rate, and photograph of the Li–SPAN pouch cell.

Table 1 | Correlation between SPAN cathodes with different compositions and thickness and reversible chg./dischg. capacities

Composition of SPAN Cathode	SPAN Layer	Capacity (mAh/g) [0.1C-rate, 30 $^{\circ}$C]
SPAN:AB:SBR:CMC-Na (92.0/5.0/1.5/1.5, wt%)	thin	686
SPAN:AB:SBR:CMC-Na (92.0/5.0/1.5/1.5, wt%)	thick	685
SPAN:AB:SBR:CMC-Na (94.0/3.0/1.5/1.5, wt%)	thin	685
SPAN:AB:SBR:CMC-Na (96.0/1.0/1.5/1.5, wt%)	thin	651
SPAN:MWCNT:SBR:CMC-Na (97.4/1.0/0.7/0.9, wt%)	thin	674
SPAN:SWCNT:SBR:CMC-Na (97.4/1.0/0.7/0.9, wt%)	thin	685
SPAN:SWCNT:SBR:CMC-Na (97.7/0.7/0.7/0.9, wt%)	thin	686
SPAN:SWCNT:SBR:CMC-Na (98.0/0.4/0.7/0.9, wt%)	thin	685
SPAN:SWCNT:SBR:CMC-Na (98.0/0.4/0.7/0.9, wt%)	thick	673
SPAN:SWCNT:SBR:CMC-Na:CNF (98.0/0.4/0.7/0.7/0.2, wt%)	thick	685

Table 2 | Correlation between electrolyte solutions and cell properties

Electrolyte Solution (chg./dischg. cycle number at 0.1C-rate and 30 ºC)	Normalized Capacity after 20 cycles	Normalized Resistance after 20 cycles
Ele-1 (20)	1.00	1.02
Ele-2 (20)	1.00	1.01
Ele-3 (20)	1.00	1.00
Ele-4 (20)	0.98	1.05
Ele-5 (20)	0.89	1.10
Ele-6 (20)　　*Ele-6 = Light-Ele	0.95	1.07
Ele-1 (5) → Ele-6 (20)　[two-step method]	0.97	1.05
Ele-2 (5) → Ele-6 (20)　[two-step method]	0.99	1.02
Ele-3 (5) → Ele-6 (20)　[two-step method]	1.00	1.00
Ele-3 (5) → Ele-4 (20)　[two-step method]	1.00	1.02
Ele-3 (5) → Ele-5 (20)　[two-step method]	0.98	1.03

Ele-1 : 1.0 M $LiPF_6$ in EC/DEC (50/50, vol%)

Ele-2 : 1.0 M $LiPF_6$ in FEC/DEC (50/50, vol%)

Ele-3 : 1.0 M $LiPF_6$ in FEC/DEC (50/50, vol%) + 2 wt% LiBOB

Ele-4 : 1.0 M LiTFSI in DOL/DME (50/50, vol%) + 2 wt% $LiNO_3$

Ele-5 : 0.4 M LiTFSI + 0.4 M $LiNO_3$ + 0.1 M LiHFDF in DME/DOL/TFMTMS (48/17/35, vol%)

Ele-6 : 0.2 M LiTFSI + 0.2 M LiFSI + 0.1 M $LiNO_3$ + 0.1 M LiHFDF in DME/DOL/TFMTMS (75/5/20, vol%)

Supplementary Files

This is a list of supplementary files associated with this preprint. Click to download.

- SupplementaryInformationNatureCommunicationskakiage20230729.pdf